Monthly Notices of the ROYAL ASTRONOMICAL SOCIETY

MNRAS **498,** 5574–5580 (2020) doi:10.1093/mnras/staa2840
Advance Access publication 2020 September 19

# Equilibrium models of the Milky Way mass are biased high by the LMC

Denis Erkal [1]★ Vasily A. Belokurov [2] and Daniel L. Parkin[1]

[1]*Department of Physics, University of Surrey, Guildford GU2 7XH, UK*
[2]*Institute of Astronomy, University of Cambridge, Madingley Road, CB3 0HA Cambridge, UK*

Accepted 2020 September 11. Received 2020 September 11; in original form 2020 January 30

## ABSTRACT

Recent measurements suggest that the Large Magellanic Cloud (LMC) may weigh as much as 25 per cent of the Milky Way (MW). In this work, we explore how such a large satellite affects mass estimates of the MW based on equilibrium modelling of the stellar halo or other tracers. In particular, we show that if the LMC is ignored, the MW mass within 200 kpc is overestimated by as much as 50 per cent. This bias is due to the bulk motion in the outskirts of the Galaxy's halo and can be, at least in part, accounted for with a simple modification to the equilibrium modelling. Finally, we show that the LMC has a substantial effect on the orbit Leo I which acts to increase its present-day speed relative to the MW. We estimate that accounting for a $1.5 \times 10^{11}\,\mathrm{M}_\odot$ LMC would lower the inferred MW mass to $\sim 10^{12}\,\mathrm{M}_\odot$.

**Key words:** Galaxy: evolution – Galaxy: halo – Galaxy: kinematics and dynamics – Magellanic Clouds.

## 1 INTRODUCTION

The Large Magellanic Cloud (LMC) is the brightest satellite of the Milky Way (MW) and has been known since antiquity (e.g. Al Sufi 1964). The first suggestion that the LMC could have a significant effect on our Galaxy was proposed by Kerr (1957) and Burke (1957) based on the observations of the deformed atomic hydrogen disc in the MW. However, calculations in those works based on the mass of the LMC at the time showed that the LMC was unlikely to explain the deformation. Avner & King (1967) followed this up with a more general exploration of the effect of the LMC. Their discussion mostly focused on how the LMC could torque and twist the disc of the MW assuming it was on a relatively circular orbit, although they also included a prescient discussion of whether or not the LMC was bound to the Small Magellanic Cloud (SMC) or to our Galaxy.

More recent work has shown that the Magellanic Clouds are likely bound to each other and are on their first approach to the MW (Kallivayalil, van der Marel & Alcock 2006; Besla et al. 2007; Kallivayalil et al. 2013). Alongside this, a number of works have shown that the LMC has a large total mass, $M_{\rm LMC} \sim 10^{11} - 2.5 \times 10^{11}\,\mathrm{M}_\odot$, based on abundance matching (e.g. Moster, Naab & White 2013), assuming the SMC was originally bound to the LMC (Kallivayalil et al. 2013), using the timing argument with Andromeda combined with the nearby Hubble flow (Peñarrubia et al. 2016), perturbations to the MW disc (Laporte et al. 2018; Gardner, Hinkel & Yanny 2020), quantifying the effect of the LMC on Orphan stream (Erkal et al. 2019), and modelling the satellites of the LMC (Erkal & Belokurov 2020).

These high LMC masses can induce a substantial reflex motion in the MW (Gómez et al. 2015) and fits to the Orphan stream predicted this could be as large as $\sim$50 km s$^{-1}$ (Erkal et al. 2019). This reflex motion should be most apparent beyond $\sim$30 kpc where the orbital periods of stars are longer than the infall time of the LMC. Along these lines, Garavito-Camargo et al. (2019) studied the effect of the LMC on the stellar halo of the MW and predicted that there should be an overdense wake behind the LMC as well as substantial non-equilibrium motion in the outskirts of our Galaxy. Belokurov et al. (2019) showed that the Pisces overdensity (Watkins et al. 2009) was consistent with this wake both in 3D shape and radial velocity. Petersen & Peñarrubia (2020) also simulated the infall of the LMC and found similar results. Thus, multiple lines of evidence suggest that the LMC has had a large effect on our Galaxy, making it significantly out of equilibrium.

In this work, we will examine how the disequilibrium of our Galaxy affects our ability to measure its mass. In particular, we will use the mass estimator from Watkins, Evans & An (2010) which assumes that our Galaxy is in equilibrium. This estimator has been used in a number of recent works to measure the mass of our Galaxy out to radii where these non-equilibrium effects are significant (e.g. Sohn et al. 2018; Watkins et al. 2019; Fritz et al. 2020). We will also explore how this reflex motion affects the mass estimate based on Leo I (Boylan-Kolchin et al. 2013). This paper is organized as follows. In Section 2, we will explore the effect of the LMC on our Galaxy and in particular how it biases the mass estimator. In Section 3, we search for the predicted reflex motion using satellites of the MW, explore how this reflex motion affects the motion of Leo I, and conclude.

## 2 EFFECT OF LMC ON THE MILKY WAY'S HALO

In order to simulate the effect of the LMC on a tracer population around the MW, we use a suite of simulations with a variety of LMC masses. The fiducial set of simulations are identical to those described in Belokurov et al. (2019). The simulations in that work are fast since the MW and LMC are not resolved with full *N*-body dynamics. Instead, they are modelled as single particles sourcing their respective potentials. The MW is modelled using the `MWPotential2014` from Bovy (2015) where the bulge is replaced by an equal mass Hernquist (1990) profile for speed. The LMC is modelled as a Hernquist profile. In this framework, the LMC is rewound from its

★ E-mail: d.erkal@surrey.ac.uk

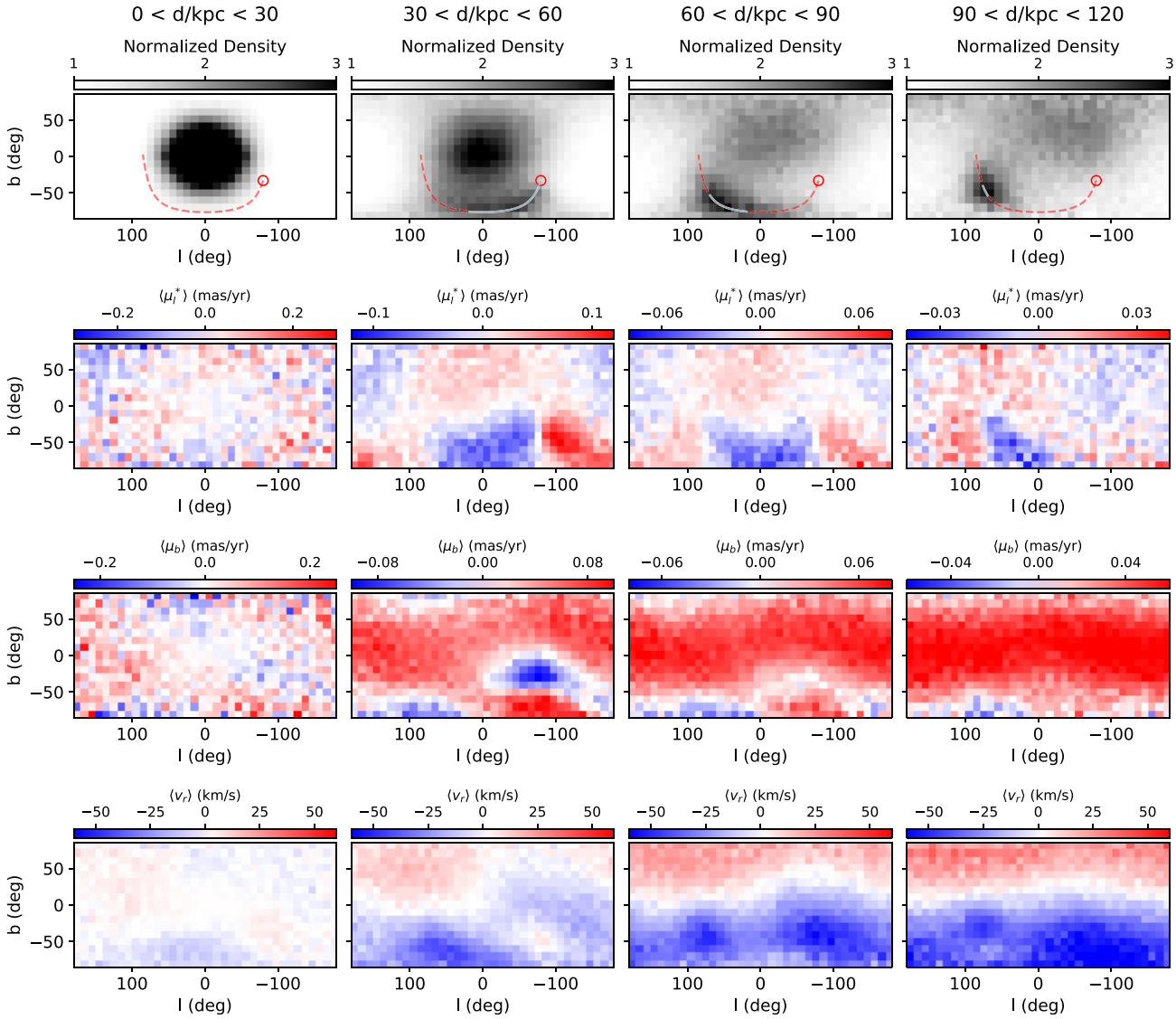


**Figure 1.** Effect of a $1.5 \times 10^{11}\,M_\odot$ LMC on the MW stellar halo in various distance bins. Each column shows a different range of distances (shown at the top of the plot). Top row shows the normalized stellar halo density. The red circle shows the present-day position of the LMC, the dashed red curve shows the past orbit of the LMC, and the light blue curve shows the section of the LMC's orbit in the given distance bin. There is a clear overdensity in the outer stellar halo which traces the past orbit of the LMC. Second row shows the mean reflex-corrected proper motion $\mu_l^*$. In the inner most distance slice, there is very little structure. However, in the more distant slices there are clear patterns in the proper motion related to the past orbit of the LMC. Third row shows the mean reflex-corrected proper motion $\mu_b$. Beyond 30 kpc, the mean proper motion is positive over most of the sky, showing that the stellar halo is moving upwards relative to the inner part of the Galaxy. Bottom row shows the mean reflex-corrected radial velocity. Beyond 30 kpc, there is a clear dipole with the halo in the Southern hemisphere having a negative radial velocity (i.e. approaching the Sun) and the halo in the Northern hemisphere having a positive radial velocity (i.e. receding from the Sun). This also shows that inner part of the Galaxy is moving downwards with respect to the outer part of the stellar halo. These results are qualitatively similar to the results in Garavito-Camargo et al. (2019).

present-day position, the stellar halo is initialized as a population of $10^7$ tracer particles with an anisotropy of $\sim$0.5 and a density profile of $\rho \propto r^{-3.5}$ at large radii (see Belokurov et al. 2019, for more details), and the system is evolved forward to the present. We assume that the Sun is located at a distance of 8.122 kpc from the Galactic centre (Gravity Collaboration et al. 2018).

Fig. 1 shows the effect of a $1.5 \times 10^{11}\,M_\odot$ LMC on the stellar halo of the MW.[1] This demonstrates that this technique gives broadly similar answers to Garavito-Camargo et al. (2019) which studied the motions of both the LMC and MW with *N*-body simulations. Comparing the two approaches it is clear that both the 'local wake' (aligned with the LMC's past orbit) and the 'global wake' (mostly in the Northern hemisphere) are reproduced. This is due to the fact that the simulations in Belokurov et al. (2019) accounted for the direct effect of the LMC on the stellar halo, as well as the reflex motion of the MW in response to the LMC. However, two key aspects missing from our simulations are the deformation of the MW and LMC in response to each other and any resonances in the MW's halo. Given that Fig. 1 closely resembles the results of Garavito-Camargo et al. (2019), these effects do

[1]The simulation output is available at https://doi.org/10.5281/zenodo.3630283

not seem to be important for the bulk properties of the stellar halo.

One key result highlighted in Fig. 1 is that the LMC induces a motion of the inner region of the MW, within roughly 30 kpc, with respect to the outer part of the Galaxy. This streaming motion is mostly in the downwards (-$z$) direction. This is apparent in the third and fourth rows of Fig. 1 which show that the distant stellar halo is moving upwards relative to the inner parts of the Galaxy. This effect was predicted in Erkal et al. (2019) which measured the mass of the LMC based on its effect on the Orphan stream. That work argued that the orbital time-scales are short in the inner part of the Galaxy and thus these stars can respond adiabatically to the LMC, while stars in the outskirts of the Galaxy, where the orbital timescales are longer, do not respond coherently, thus giving rise to a bulk motion. Since the LMC's past orbit has most recently been below the MW, the Cloud can be seen as pulling the inner part of the MW downwards. This effect was also seen in the simulations in Garavito-Camargo et al. (2019).

This streaming motion suggests that equilibrium modelling will likely be biased in the presence of the LMC. To quantify this systematic error, we focus on the mass estimator from Watkins et al. (2010) which makes use of the tracers 3D velocity. This has been used in several recent works (e.g. Sohn et al. 2018; Watkins et al. 2019; Fritz et al. 2020) but due to the streaming motion relative to the outskirts of our Galaxy, we expect that any method which assumes dynamical equilibrium will be biased. This estimate is given by

$$M = \frac{\alpha + \gamma - 2\beta}{3 - 2\beta} \frac{r_{\rm out}^{1-\alpha}}{G} \langle v^2 r^{\alpha} \rangle, \quad (1)$$

where $\alpha$ is the power-law slope of the potential (i.e. $\psi(r) \propto r^{-\alpha}$), $\beta$ is the anisotropy of the tracer population, $\gamma$ is the power-law slope of the tracer density (i.e. $\rho \propto r^{-\gamma}$), $r$ is the galactocentric distance to each tracer, $v^2$ is the 3D speed of each tracer relative to the Galaxy, and $r_{\rm out}$ is the radius of the outermost tracer.

We apply this mass estimator to the simulated stellar haloes from Belokurov et al. (2019). In particular, we use the $5 \times 10^{10}$, $1.5 \times 10^{11}$, and $2.5 \times 10^{11}$ $M_\odot$ LMC runs and the run with no LMC. First, as a reference, we use equation (1) to measure the MW mass in the simulation without the LMC. For this stellar halo, we expect that the estimator in equation (1) will recover the true mass profile. We break the stellar halo into radial bins from 30 to 200 kpc. For each bin, we use a bin width which is ∼19 per cent of the radius so that the mass estimate is as accurate as possible. This results in 10 bins in the range 30–200 kpc. If we use significantly larger bins, then the power-law slope of the potential and tracer density can change significantly within each bin, making the estimator less precise. The results are shown in Fig. 2. The green circles show the mass estimator applied to the simulation with no LMC. As expected, this faithfully reproduces the true mass distribution of the simulated MW.

Next we consider the simulations with three different LMC masses. The resulting mass profiles are also shown in Fig. 2 using different colour symbols. As the LMC mass is increased, the MW mass is progressively overestimated. Indeed, at 200 kpc, this can result in an up to ∼ 50 per cent overestimate of the MW mass. Interestingly, all of the measurements converge to the true MW mass within ∼30 kpc since within this region there is no significant bulk motion and the MW is effectively in equilibrium.

We note that this bias will depend on the mass of the MW as well. To show this, we increased the virial MW halo mass by 50 per cent (to $1.2 \times 10^{12}$ $M_\odot$) and repeated the analysis for a $1.5 \times 10^{11}$ $M_\odot$ LMC. We found that the bias at 200 kpc reduced to ∼ 13 per cent from the ∼ 25 per cent bias seen in the fiducial setup. That said, the fiducial setup has a MW potential broadly similar to what was inferred with the Orphan stream (Erkal et al. 2019) and thus should be a good reflection of the actual bias for the MW.

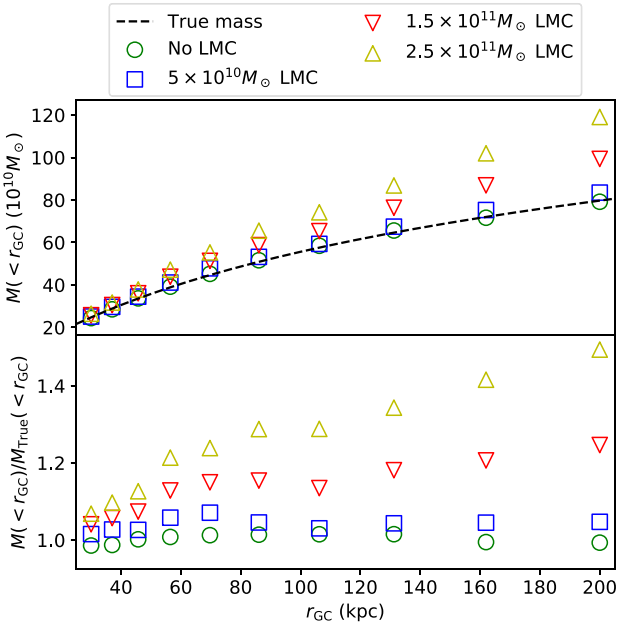


**Figure 2.** Mass estimator applied to simulated MW in the presence of the LMC. Top panel shows the mass estimator applied to four simulations with various LMC masses. The simulation with no LMC matches the true mass quite well, while as the LMC mass is increased, the inferred mass is increasingly biased. As expected, the estimates converge to the true value within ∼ 30 kpc since the MW does not have any bulk motion within this region. Bottom panel shows the inferred mass divided by the true mass, that is, the size of the bias. For the most massive LMC considered here, $2.5 \times 10^{11}$ $M_\odot$, the inferred mass is ∼ 50 per cent higher than the true mass at 200 kpc. However, even at more modest radii of ∼ 50 kpc, this bias can reach 20 per cent.

In Fig. 3, we explore the bulk velocity induced by the LMC's in-fall by computing the tracer mean velocity in radial shells. If the LMC is not included, the mean velocity is close to zero as expected since the stellar halo is in equilibrium. However, as the LMC mass is increased, the mean velocity grows significantly in the outer parts of the halo ($r >$ ∼30 kpc). The bulk motion of the distant stellar halo is mostly in the upwards (i.e. +$z$-direction). This is due to the fact that in the recent past, the LMC's orbit has taken it below the plane of the MW. As the Cloud passes its pericentre, the short orbital time-scales in the inner part of the MW allow it to respond coherently, while the timescales in the outer part are too long. Thus, the inner part of the MW is accelerated downwards relative to the outer parts as argued in Erkal et al. (2019).

The simulations in Belokurov et al. (2019) were tailored to be similar to the stellar halo since they have an anisotropy of ∼0.5 in agreement with recent measurements in the Galaxy (see e.g. Lancaster et al. 2019). In order to study how other tracer populations, that is, globular clusters or dwarf galaxies, are affected we run two additional simulations. For these, we have an anisotropy of ∼0 and ∼−0.5 to investigate how changing the anisotropy affects our results. As in Belokurov et al. (2019), the initial conditions are generated using AGAMA (Vasiliev 2019a) with the `DoublePowerLaw` distribution functions from Posti et al. (2015). For an anisotropy of ∼ 0, we use `norm = 1.5e10, j0 = 500, slopeIn = 0, slopeOut = 3.5, coefJrOut = 1.175,`

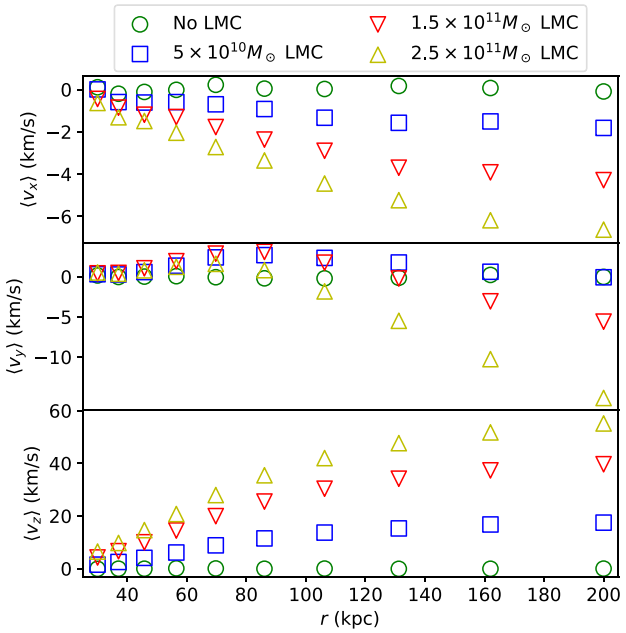


**Figure 3.** Magnitude of mean velocity in radial shells in the presence of various mass LMCs. If the LMC is not included, the mean velocity in all shells is close to zero, as expected if the system is in equilibrium. However, as the LMC mass is increased, the mean velocity beyond ∼30 kpc increases to nearly 60 km s$^{-1}$ in the case of the $2.5 \times 10^{11}$ M$_\odot$ LMC. The velocity is mainly in the $+z$-direction (i.e. upwards): over the radial range considered here, the velocity is always within ∼18° of the $+z$- direction. This large bulk velocity shows that the outer parts of the stellar halo are significantly out of equilibrium due to the LMC. Note that the $y$-range of each panel is different.

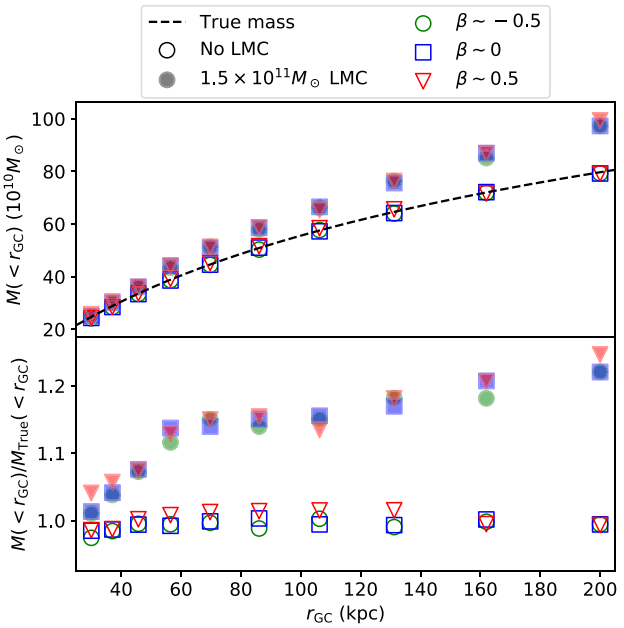


**Figure 4.** Mass estimator applied to stellar haloes with various anisotropies in the presence of the LMC. Top panel shows the mass estimator compared to the true mass and the bottom panel shows the mass estimator divided by the true mass. Since the anisotropy does not significantly affect the mass estimate, the bias induced by the LMC should be present in all tracer populations.

`coefJzOut = 0.9125, jcutoff = 1e5, cutoffStrength = 2` and for an anisotropy of ∼ −0.5, we use `norm = 1.5e10, j0 = 500, slopeIn = 0, slopeOut = 3.5, coefJrOut = 1.48, coefJzOut = 0.76, jcutoff = 1e5, cutoffStrength = 2`. For these different anisotropies, we only consider an LMC mass of $1.5 \times 10^{11}$ M$_\odot$. In Fig. 4, we compare the mass estimator with three different anisotropy values and see that the estimator is similarly biased, independent of the anisotropy chosen. Thus, we should expect that estimates of the MW with any tracer will be strongly affected.

Since a lot of the velocity structure in Fig. 1 appears to be due to the inner part of the Galaxy moving downwards with respect to the outer parts, we propose a slightly modified version of the estimator from Watkins et al. (2010) which uses the velocity dispersion relative to the mean velocity:

$$M_{\bar{v}} = \frac{\alpha + \gamma - 2\beta}{3 - 2\beta} \frac{r_{\rm out}^{1-\alpha}}{G} \langle (\mathbf{v} - \bar{\mathbf{v}})^2 r^\alpha \rangle. \quad (2)$$

A comparison of this estimator versus the one in equation (1) is shown in Fig. 5 for eight different octants (marked according to their positive or negative position along each of $y$-, $z$-, $x$-axes, or equivalently $l$, $b$, $x$). Two of the best octants are (−, +, −) and (−, +, +). These correspond to $l < 0°$ and $b > 0°$. Referring back to Fig. 1, this is reassuringly the quadrant of the sky with the least structure in the velocity.

In Appendix A, we compare the result of the mass estimator with the total enclosed mass of the MW and LMC. While we find a smaller bias, we argue that the mass estimator should not be thought of as measuring the LMC mass since the LMC has not yet merged and phase mixed with our Galaxy. Instead we argue that the corrected

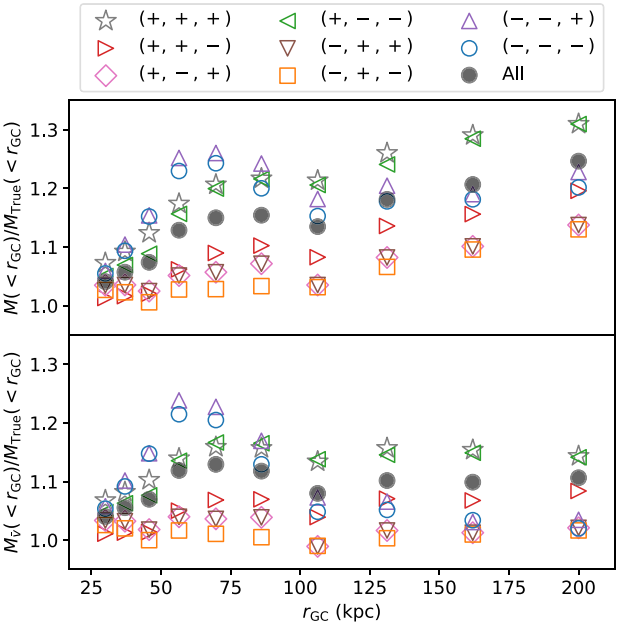


**Figure 5.** Mass estimator applied on different octants in the presence of a $1.5 \times 10^{11}$ M$_\odot$ LMC. Top panel shows the mass estimator applied on the octants of the MW's standard galactocentric Cartesian coordinates. The octants are specified in the legend by the sign of the $y$, $z$, $x$ coordinates (equivalently $l$, $b$, $x$ coordinates) respectively, for example, (+, +, +) means $y > 0$, $z > 0$, $x > 0$, or equivalently, $l > 0$, $b > 0$, $x > 0$. Given the velocity structure apparent in Fig. 1, it is not surprising that the mass estimator applied to the various octants gives a different result. While the majority of the most biased octants are in the Southern hemisphere (i.e. $z < 0$), the octant (+, +, +) is also significantly biased. Bottom panel shows the mass estimator which accounts for the bulk velocity of the tracers (see equation 2). Several octants can now provide an unbiased estimate over a wide range of radii, especially octants (−, +, +), (−, +, −), (+, −, +), and (slightly worse) (+, +, −).

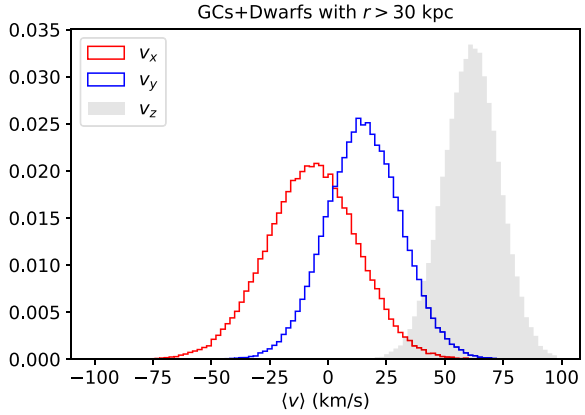


**Figure 6.** Mean velocity in sample of 33 globular clusters and dwarfs with Galactocentric distances larger than 30 kpc. This shows that these satellites have a substantial velocity shift relative to the MW. This could be due to the reflex motion induced by the LMC or due to substructure and phase-space correlation amongst the satellites.

mass estimator (i.e. computed with equation 2) should be thought of as measuring the MW mass.

## 3 DISCUSSION AND CONCLUSIONS

### 3.1 Search for velocity shift in the observations

In Fig. 1, we showed that the LMC has a large effect on the outer parts of the MW. One of the main results is that the outer regions of the MW are moving upwards relative to the inner regions. In order to test this, we use a sample of 33 globular clusters and dwarf galaxies with Galactocentric radii larger than 30 kpc. The data for the globular clusters come from Vasiliev (2019b), and references therein. Since no distance error is provided, we assume an error of 5 per cent for each globular cluster which corresponds to a distance modulus error of 0.1 mag (e.g. Gratton et al. 2003; Correnti et al. 2018). The data for the ultrafaint dwarfs come from Simon & Geha (2007), Koposov et al. (2011), Willman et al. (2011), Kirby et al. (2013, 2017), Martin et al. (2016), Walker et al. (2016), Simon et al. (2017), Simon (2018), Pace & Li (2019), and Torrealba et al. (2019). For the classical dwarfs, we use the observed values from Gaia Collaboration et al. (2018) as well as proper motions for Leo I and Leo II from Sohn et al. (2013) and Piatek, Pryor & Olszewski (2016), respectively. In order to avoid any obvious clustering, we exclude the dwarfs associated with the LMC, including the LMC and SMC (Kallivayalil et al. 2018; Erkal & Belokurov 2020; Patel et al. 2020).

For this sample, we then make 100 000 Monte Carlo realizations of their Cartesian velocities (given the observables and their uncertainties) and compute the mean of each Cartesian velocity. We note that the cut at 30 kpc is made after each Monte Carlo realization, that is, some satellites only contribute in a fraction of the realizations. The distributions of these means are shown in Fig. 6 where we see that while $v_x$ and $v_y$ have means which are consistent with zero, the mean of $v_z$ is significantly non-zero and positive. This is in line with the predicted effect of the LMC (see Fig. 3). For completeness, we repeated this analysis with only the globular clusters beyond 30 kpc and only the dwarfs beyond 30 kpc and found that the result was much less significant, likely due to the shot noise from the smaller number of satellites. As a caveat, we also note that since satellites are known to arrive to the MW in associations, it is possible that this signal is due to recently accreted groups of dwarf galaxies which have not yet phase mixed in their orbits around the MW. Future observations of the stellar halo with a much larger set of tracers will verify whether this signal is real and, if so, whether it is due to the LMC.

Along similar lines, we note that Gilbert et al. (2018) have shown that there is a significant velocity offset between the stellar halo and disc in Andromeda (see fig. 7 of that work). Such an offset could arise from an interaction between Andromeda and a large satellite as in this work. Thus, this may be due to the recent merger proposed by Hammer et al. (2018).

### 3.2 Leo I

The large relative speed of the Leo I dwarf galaxy relative to the MW (Sohn et al. 2013) has been used to constrain the mass of the MW (Boylan-Kolchin et al. 2013) assuming that it is bound to our Galaxy. However, since the outer parts of our Galaxy are out of equilibrium, this relative speed already includes the additional reflex motion imparted by the LMC. In order to assess the impact of the LMC on Leo I, we take two approaches. First, we estimate this reflex motion using the fiducial simulations from Section 2 with an LMC mass of $1.5 \times 10^{11}\,\mathrm{M}_\odot$. We take the mean velocity of all particles within 2° on the sky and 30 kpc along the line of sight from the currently measured location of Leo I. Accounting for the reflex motion, the relative speed of Leo I drops from ∼197 to ∼168 km s$^{-1}$.

Second, we integrate the orbit of Leo I in the presence of the LMC using the machinery from Erkal & Belokurov (2020). Namely, we rewind Leo I back in time for 5 Gyr (or until the LMC has an apocentre, whichever is sooner) including the effect of a $1.5 \times 10^{11}\,\mathrm{M}_\odot$ LMC. The MW and LMC potentials are the same as in Section 2. We Monte Carlo the present-day positions and velocities of the LMC and Leo I 10 000 times and compare the energy of Leo I relative to the MW at the present and 5 Gyr ago (i.e. before the infall of the LMC). We find that the energy of Leo I was substantially lower (i.e. it was substantially more bound) before the infall of the LMC. In order to facilitate the comparison with Boylan-Kolchin et al. (2013), we convert this energy difference into a change of the velocity of Leo I. Thus, we find that if Leo I was observed at its current location before the infall of the LMC, it would have had a speed of ∼169 km s$^{-1}$ relative to the MW. This is much lower than its present-day relative speed of ∼197 km s$^{-1}$.

Interestingly, both approaches give nearly the same result showing consistently that a significant portion of Leo I's speed is due to the LMC. In terms of the results of Boylan-Kolchin et al. (2013), this ∼ 15 per cent decrease in the speed is a slightly larger effect than changing the MW mass from $10^{12}$ to $1.5 \times 10^{12}\,\mathrm{M}_\odot$ which results in a ∼ 13 per cent reduction in $v/v_{\rm vir}$. This suggests that if the analysis of Boylan-Kolchin et al. (2013) was repeated accounting for a $1.5 \times 10^{11}\,\mathrm{M}_\odot$ LMC, the inferred MW mass would be close to $\sim 10^{12}\,\mathrm{M}_\odot$.

### 3.3 Conclusions

In this work, we have shown that the LMC should push the outskirts of our Galaxy substantially out of equilibrium. In particular, the leading order effect of the LMC is that the inner parts of the MW nearly decouple from the region beyond ∼30 kpc. Thus, observations of populations beyond ∼30 kpc should show signs of this near-bulk motion. Importantly, we demonstrated how this disequilibrium affects models of matter distribution in the outer parts of our Galaxy using the mass estimator of Watkins et al. (2010). The systematic bias in the tracer velocity dispersion induces the mass bias which depends on radius but is always positive (e.g. Fig. 2). For the MW mass

enclosed within 200 kpc, this bias can be as large as $\sim 50$ per cent, depending on the mass of the LMC. We note that in this work we neglected the effect of substructure in the stellar halo which can cause mass estimates to be biased low by as much as $\sim 40$ per cent (e.g. Yencho et al. 2006; Wang et al. 2015). This bias will partially offset the bias due to the LMC although future work is needed to test the interplay of these effects.

We showed that the bias due to the LMC depends on where the tracers are located and that certain parts of the sky offer a substantially improved estimate. This bias can also be reduced if the mean reflex motion is accounted for. As an application of this idea, we showed that the LMC significantly increases the present-day speed of Leo I relative to the MW and that if this is accounted for, the MW mass estimate of Boylan-Kolchin et al. (2013) will be significantly lower.

Accounting for the reflex motion induced by the LMC may also bring into closer agreement the different mass estimates for the MW (e.g. Bland-Hawthorn & Gerhard 2016; Wang et al. 2020) which are made with tracers at different radii and using different techniques. Based on the results of this work, the estimates made with data in the outskirts of our Galaxy are likely biased high due to the nearly bulk motion beyond ~30 kpc. Future observations of the stellar halo with *Gaia* DR3, as well as upcoming radial velocity surveys like WEAVE and 4MOST, will allow us to measure this bulk motion and determine how significant this effect is.

## ACKNOWLEDGEMENTS

We thank the referee for their helpful comments which improved the clarity of this work. We thank Alis Deason, Tobias Fritz, Jiaxin Han, and Qingyang Li for questioning whether or not the LMC's mass should be included with the MW mass. We thank Wyn Evans for helpful comments while preparing the manuscript. We thank Eugene Vasiliev for help with using AGAMA. This research made use of IPYTHON (Perez & Granger 2007), PYTHON packages NUMPY (van der Walt, Colbert & Varoquaux 2011), MATPLOTLIB (Hunter 2007), and SCIPY (Jones et al. 2001). This research also made use of ASTROPY,[2] a community-developed core PYTHON package for Astronomy (Astropy Collaboration et al. 2013; Price-Whelan et al. 2018).

## DATA AVAILABILITY

The present-day snapshot of the fiducial simulation with an LMC mass of $1.5 \times 10^{11}\,M_{\odot}$ is publicly available at https://doi.org/10.5281/zenodo.3630283. All other simulation outputs will be shared on reasonable request to the corresponding author.

## REFERENCES

Al Sufi A., 1964, Book of Fixed Stars. Isfahan, Persia
Astropy Collaboration et al., 2013, A&A, 558, A33
Avner E. S., King I. R., 1967, AJ, 72, 650
Belokurov V., Deason A. J., Erkal D., Koposov S. E., Carballo-Bello J. A., Smith M. C., Jethwa P., Navarrete C., 2019, MNRAS, 488, L47
Besla G., Kallivayalil N., Hernquist L., Robertson B., Cox T. J., van der Marel R. P., Alcock C., 2007, ApJ, 668, 949
Bland-Hawthorn J., Gerhard O., 2016, ARA&A, 54, 529
Bovy J., 2015, ApJS, 216, 29
Boylan-Kolchin M., Bullock J. S., Sohn S. T., Besla G., van der Marel R. P., 2013, ApJ, 768, 140
Burke B. F., 1957, AJ, 62, 90
Correnti M., Gennaro M., Kalirai J. S., Cohen R. E., Brown T. M., 2018, ApJ, 864, 147
Erkal D., Belokurov V. A., 2020, MNRAS, 495, 2554
Erkal D. et al., 2019, MNRAS, 487, 2685
Fritz T. K., Di Cintio A., Battaglia G., Brook C., Taibi S., 2020, MNRAS, 494, 5178
Gaia Collaboration et al., 2018, A&A, 616, A12
Garavito-Camargo N., Besla G., Laporte C. F. P., Johnston K. V., Gómez F. A., Watkins L. L., 2019, ApJ, 884, 51
Gardner S., Hinkel A., Yanny B., 2020, ApJ, 890, 110
Gilbert K. M. et al., 2018, ApJ, 852, 128
Gómez F. A., Besla G., Carpintero D. D., Villalobos Á., O'Shea B. W., Bell E. F., 2015, ApJ, 802, 128
Gratton R. G., Bragaglia A., Carretta E., Clementini G., Desidera S., Grundahl F., Lucatello S., 2003, A&A, 408, 529
Gravity Collaboration et al., 2018, A&A, 615, L15
Hammer F., Yang Y. B., Wang J. L., Ibata R., Flores H., Puech M., 2018, MNRAS, 475, 2754
Hernquist L., 1990, ApJ, 356, 359
Hunter J. D., 2007, Comput. Sci. Eng., 9, 90
Jones E. et al., 2001, SciPy: Open Source Scientific Tools for Python. Available at: http://www.scipy.org/ (Last accessed: September 11, 2019)
Kallivayalil N., van der Marel R. P., Alcock C., 2006, ApJ, 652, 1213
Kallivayalil N., van der Marel R. P., Besla G., Anderson J., Alcock C., 2013, ApJ, 764, 161
Kallivayalil N. et al., 2018, ApJ, 867, 19
Kerr F. J., 1957, AJ, 62, 93
Kirby E. N., Boylan-Kolchin M., Cohen J. G., Geha M., Bullock J. S., Kaplinghat M., 2013, ApJ, 770, 16
Kirby E. N., Cohen J. G., Simon J. D., Guhathakurta P., Thygesen A. O., Duggan G. E., 2017, ApJ, 838, 83
Koposov S. E. et al., 2011, ApJ, 736, 146
Lancaster L., Koposov S. E., Belokurov V., Evans N. W., Deason A. J., 2019, MNRAS, 486, 378
Laporte C. F. P., Gómez F. A., Besla G., Johnston K. V., Garavito-Camargo N., 2018, MNRAS, 473, 1218
Martin N. F. et al., 2016, MNRAS, 458, L59
Moster B. P., Naab T., White S. D. M., 2013, MNRAS, 428, 3121
Pace A. B., Li T. S., 2019, ApJ, 875, 77
Patel E. et al., 2020, ApJ, 893, 121
Peñarrubia J., Gómez F. A., Besla G., Erkal D., Ma Y.-Z., 2016, MNRAS, 456, L54
Perez F., Granger B. E., 2007, Comput. Sci. Eng., 9, 21
Petersen M. S., Peñarrubia J., 2020, MNRAS, 494, L11
Piatek S., Pryor C., Olszewski E. W., 2016, AJ, 152, 166
Pietrzyński G. et al., 2013, Nature, 495, 76
Posti L., Binney J., Nipoti C., Ciotti L., 2015, MNRAS, 447, 3060
Price-Whelan A. M. et al., 2018, AJ, 156, 123
Simon J. D., 2018, ApJ, 863, 89
Simon J. D., Geha M., 2007, ApJ, 670, 313
Simon J. D. et al., 2017, ApJ, 838, 11
Sohn S. T., Besla G., van der Marel R. P., Boylan-Kolchin M., Majewski S. R., Bullock J. S., 2013, ApJ, 768, 139
Sohn S. T., Watkins L. L., Fardal M. A., van der Marel R. P., Deason A. J., Besla G., Bellini A., 2018, ApJ, 862, 52
Torrealba G. et al., 2019, MNRAS, 488, 2743
van der Walt S., Colbert S. C., Varoquaux G., 2011, Comput. Sci. Eng., 13, 22
Vasiliev E., 2019a, MNRAS, 482, 1525
Vasiliev E., 2019b, MNRAS, 484, 2832
Walker M. G. et al., 2016, ApJ, 819, 53
Wang W., Han J., Cooper A. P., Cole S., Frenk C., Lowing B., 2015, MNRAS, 453, 377
Wang W., Han J., Cautun M., Li Z., Ishigaki M. N., 2020, Sci. China Phys. Mech. Astron., 63, 109801

[2] http://www.astropy.org

Watkins L. L. et al., 2009, MNRAS, 398, 1757
Watkins L. L., Evans N. W., An J. H., 2010, MNRAS, 406, 264
Watkins L. L., van der Marel R. P., Sohn S. T., Evans N. W., 2019, ApJ, 873, 118
Willman B., Geha M., Strader J., Strigari L. E., Simon J. D., Kirby E., Ho N., Warres A., 2011, AJ, 142, 128
Yencho B. M., Johnston K. V., Bullock J. S., Rhode K. L., 2006, ApJ, 643, 154

## APPENDIX A: INCLUDING THE LMC MASS AS PART OF THE MILKY WAY

Throughout this work, we have compared the result of the mass estimator to the enclosed mass of the MW. However, since the LMC is currently ∼50 kpc from the MW (Pietrzyński et al. 2013), the majority of its dark matter content is well within 200 kpc and thus could already be considered as part of the MW. In Fig. A1, we compare the result of the mass estimator with the enclosed mass of the LMC with the MW. Comparing this with Fig. 2, we see that the bias is smaller although still significant, especially at large radii and high LMC masses. This modest improvement could be used to argue that the mass estimator applied on the stellar halo is measuring the present-day combined MW and LMC mass. Such an argument would definitely be valid once the LMC has merged with the MW and the resulting debris has had time to phase mix. However, the LMC has only recently completed its first approach to the MW and thus neither its' nor the MW's dark matter is in equilibrium with our Galaxy. Indeed, even in the idealized setup here where we neglect the deformation of the MW and LMC, the estimator does not robustly measure the combined MW and LMC mass. We suggest a better approach is to think of the mass estimator (suitably corrected as in Fig. 5) as measuring the MW mass before the LMC's infall.

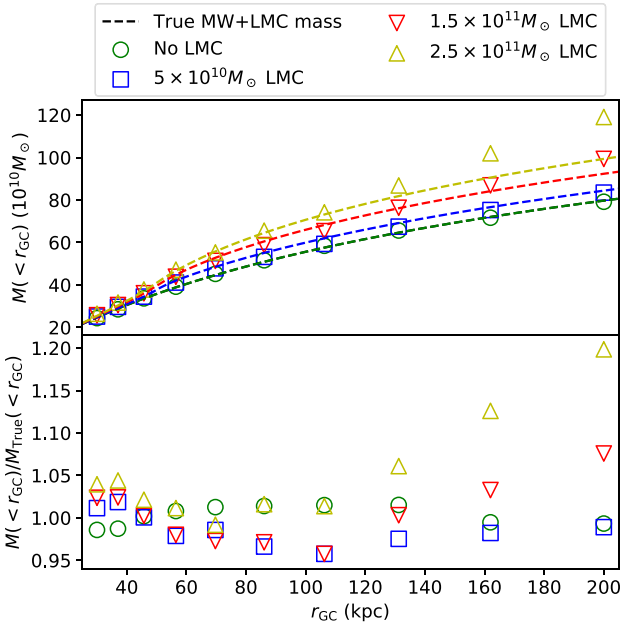


**Figure A1.** Mass estimator applied to simulated MW in the presence of the LMC. This figure is similar to Fig. 2 except we now take the true mass to be the enclosed mass of the MW and LMC. Top panel shows the mass estimator applied to four simulations with various LMC masses. The different colour curves correspond to the different LMC masses and show the total enclosed mass of the MW and LMC. Including the LMC gives a closer agreement to the enclosed mass. Bottom panel shows the inferred mass divided by the true mass, that is, the mass of the MW and LMC. Compared to Fig. 2, we see that the agreement is much better although a substantial bias still remains at large radii if the LMC is sufficiently massive.

This paper has been typeset from a TEX/LATEX file prepared by the author.